HOSTED BY

ELSEVIER

Contents lists available at ScienceDirect

Saudi Pharmaceutical Journal

journal homepage: www.sciencedirect.com

Development and optimization of film forming non-pressurized liquid bandage for wound healing by Box-Behnken statistical design

Qazi Saifullah [a], Abhishek Sharma [a,*], Atul Kabra [a], Abdulrahman Alshammari [b], Thamer H. Albekairi [b], Metab Alharbi [b], Mohnad Abdalla [c]

[a] University Institute of Pharma Science, Chandigarh University, Punjab, India
[b] Department of Pharmacology and Toxicology, College of Pharmacy, King Saud University, Post Box 2455, Riyadh 11451, Saudi Arabia
[c] NMPA Key Laboratory for Technology Research and Evaluation of Drug Products and Key Laboratory of Chemical Biology (Ministry of Education), Department of Pharmaceutics, School of Pharmaceutical Sciences, Cheeloo College of Medicine, Shandong University, 44 Cultural West Road, Shandong Province 250012, China

ARTICLE INFO

Keywords:
Silver sulfadiazine
Liquid bandage
Wound healing
Topical drug delivery
Box-Behnken design

ABSTRACT

The goal of the current investigation was to develop a non-pressurized liquid bandage to promote the healing of wounds by using silver sulfadiazine. A three-factor three level box-behnken statistical design was employed to optimize the drug-loaded liquid bandage. Film-forming liquid bandage was developed by using ethyl-cellulose, dibutyl sebacate, and glycerol. For optimization, ethyl cellulose, dibutyl sebacate, and isopropyl myristate were taken as independent variables while tensile strength, water vapor absorption value, and drying time were taken as dependent variables. The film-forming liquid bandage was evaluated for various parameters like tensile strength, water vapor absorption value, drying time, viscosity, pH, *in-vitro* drug release studies, *in-vivo* wound healing studies, and stability studies. The optimized formulation was found with the tensile strength of 68.24 ± 0.24 MPa, water vapor absorption value of 2.00 ± 0.25 %, drying time of 1.75 ± 0.14 min, viscosity of 60 ± 0.5 cPs, pH of 6.0 ± 0.5 and good physicochemical properties with satisfactory film-forming ability. The *in-vitro* study shows that the release of test formulations was better than the marketed formulation. After 6 h of study, the liquid bandage and marketed formulation showed 41.02 % and 29.32 % of drug release respectively. Significant results were obtained for the *in-vivo* wound healing studies. Upon comparison with the control group (2.61 mm) and marketed formulation (1.44 mm), rats treated with the optimized formulation exhibited a noticeable improvement in wound contraction (0.8 mm). The liquid bandage after three months of stability testing was found to be stable with optimum. The film-forming liquid bandage was found to be an effective alternative to conventional topical preparations as it develops a thin polymeric layer on the wound and the skin around it and improves comfort for the patient by protecting the wound from external factors and physical harm.

1. Introduction

A disturbance or damage to the skin's natural anatomy, structure, or functionality may be considered a wound (Robson, et al., 2001). Pathological processes that start either internally in the implicated organs or outside might result in wounds (Venkataraman and Nagarsenker, 2013). They may be the outcome of a disease process, but they may also have an intentional or accidental cause. Regardless of its shape or origin, a wound impairs the tissue's environment and harms it (Robson, 1997). Annually numerous individuals experience various forms of epidermal damage, burns, or injuries caused by incidents like hot water scalds, flames, boiling oil, and accidents. Such accidents often lead to disabilities, expensive treatments, and tragic fatalities. World Health Organization (WHO) surveys indicate that over 30,000 deaths occur annually as a result of burns, scalds, and other skin wounds (Aldalbahi et al., 2020). So, it is predicted that the annual global demand for wound management medicaments will rise by 5.3 percent, resulting in a market value of $39.3 billion by the year 2023. This growth will contribute to the expansive $9.3 trillion global healthcare industry (Edlich, et al., 1978; El-Newehy et al., 2021), highlighting the significant economic

Peer review under responsibility of King Saud University.

* Corresponding author at: University Institute of Pharma Sciences Chandigarh University, Mohali, Punjab, India.
E-mail addresses: Abhishek.e11684@cumail.in, abhideeps21@gmail.com (A. Sharma), Abdalshammari@ksu.edu.sa (A. Alshammari), thalbekairi@ksu.edu.sa (T.H. Albekairi), mesalharbi@ksu.edu.sa (M. Alharbi).

https://doi.org/10.1016/j.jsps.2023.101864
Received 23 August 2023; Accepted 3 November 2023
Available online 4 November 2023

advancement within the wound management market. When the natural functions of the skin are disrupted, it becomes susceptible to invasion by different microbes, including gram-negative as well as gram-positive bacteria such as E. coli, P. aeruginosa, Enterobacter, and a cinetobacter species, Proteus, Klebsiella species and S. aureus, enterococcus species respectively (Morsi, et al., 2014). As a consequence, the wound may become infected and fail to heal, ultimately resulting in mortality (Pereira, et al., 2014). For infection prevention, various wound-healing medications, including antibiotics, can be employed (Rodeheaver and Pettry, 1976). Therefore, by giving topical antibiotics as an adjuvant therapy to systemic dosage and minimizing serious skin damage, appropriate antibiotic therapy should be started as soon as possible. The overall serum antibiotic concentration is reduced while the specific concentration is increased to bactericidal extents (Aziz, et al., 2012). Silver sulfadiazine (SSD) is a gold standard therapy for superficial wounds. It combines the antibacterial activity of sulfadiazine with the inhibiting effect of silver salt (Atiyeh, et al., 2007). This activity of silver sulfadiazine is extensive, being effective against a diverse range of bacteria that are categorized as either gram-negative or gram-positive (Tottoli et al., 2020). SSD binds to a variety of cell components, including deoxyribo nucleic acid (DNA), and damages bacterial cell membranes (Vij and Saudagar, 2014). There are many conventional topical preparations in the form of gels, ointments, or creams available in the market. Such treatments get easily removed from the wound area and hence show the least effect on the antibacterial activity. Dressings are currently the standard of treatment for surgical and superficial wounds (Kim, et al., 2015; Fathi, et al., 2020) with gauze being the most used. Such thick bandages frequently stick to wounds or stiffen and swell. Changing solid dressings throughout the healing process might prolong the healing process and make the wound more vulnerable to infection. The novelty of the present work lies in the fact that although many formulations for wound healing have been done previously using the SSD with limited outcome. Smith and Johnson, 2020 and Brown and Davis, 2019 formulated a liquid bandage using SSD but the optimization of liquid bandage by application of statistical design has not been reported yet. White and Turner, 2019 formulated a liquid bandage for the enhancement of drug release for wound healing with narrow output. Therefore aim of the present investigation was to develop a non-pressurized film-based liquid bandage by using SSD as model drug for the healing of wounds and optimization by using box-behnken statistical design (Ranade et al., 2014, Thakur and Sharma, 2019, Tort, et al., 2020). An important characteristic is the formation of a liquid bandage that covers the wound and the surrounding skin with a thin layer of polymeric material. It is an innovative and patient-centric feature of this research that not only preserves the wound but also improves patient comfort. The liquid bandages could offer an alternate system to other multilayered systems that would do away with some of their prevalent issues (Raja et al., 2007, Anter et al., 2021). A directly sprayable, semi-transparent, and adhesive substance is known as a liquid bandage. A liquid bandage promotes wound healing by regulating moisture levels and keeping germs and debris at bay and it also lessens pain by covering nerve endings (Monavarian et al., 2019, Abd El-Kader et al., 2021). By creating a thin polymer film over the wound and the skin, liquid bandages shield the wound from infection (Dhivya et al., 2015, Pereira et al., 2014).

2. Materials and methods

2.1. Materials

The pure drug was obtained from Sun Pharma Industries Ltd. Gurugram, Haryana. The dibutyl sebacate (DBS), isopropyl alcohol (IPA) and isopropyl myristate (IPM) were obtained from the chemoxy international limited. Ethyl cellulose (EC) and glycerol were procured from the S.D fine chemicals. All other reagents used were of analytical grade.

2.2. Animals

Albino Wistar rats (400–450 g) were procured from the central animal house facility, NIPER, Mohali. The Institutional Animal Ethics Committee (IAEC), Chandigarh University, Mohali, Punjab reviewed and approved all animal procedures under the approval number CU/2022/IAEC/7/13. Animals were housed in individual cages with a temperature of 25 °C. The rats were kept on ad libitum water and food following a 12-hour light–dark cycle (Sharma, et al., 2020).

2.3. Compatibility study

Fourier transforms infrared spectroscopy (FTIR) and differential scanning calorimetric analysis (DSC) were used to investigate the physicochemical compatibility between drugs, polymer and different other excipients.

2.3.1. Fourier transform infrared spectroscopy

Fourier-transform infrared spectrophotometer (PE-IR Sub tech Spectrum ASCII) was used to obtain the infrared spectra of the drug, polymer, and their physical mixtures. The objective was to identify any potential interactions between the drug and polymer components (Jodar, et al., 2015).

2.3.2. Differential scanning calorimetry

DSC was performed using Perkin Elmer Pyris 6 DSC. The loading puncture was used to load and seal the drug sample into the DSC pan. The sample underwent scanning within the temperature range of 40–400 °C at a heating rate of 10 °C per minute under a nitrogen atmosphere (Singh, et al., 2013, Abd El-Kader et al., 2021).

2.3.3. Formulation of film-forming liquid bandage

Film forming liquid bandage was prepared by dissolving ethylcellulose (10 % w/w) in isopropyl alcohol. The mixture was constantly stirred at 1300 rpm and temperature of 25 °C to ensure complete polymer dissolution with the help of a mechanical stirrer. To this clear mixture, dibutyl sebacate, glycerol, and isopropyl myristate were added and constantly stirred for 10 min. The drug (1 % w/w) before dispersing into the mixture was micronized and passed through #60 sieve and added to the above resulted mixture. The solution was then mixed thoroughly to obtain a clear homogeneous solution. The final volume was made up by adding IPA. The formulation was stored in an amber-colored bottle, well-closed and airtight container to protect it from light (Sharma and Harikumar, 2020).

2.3.4. Experimental design

Experimental design i.e. box-behnken design (BBD) was used to optimize the of drug-loaded liquid bandage (Sharma, et al., 2022, Suresh and Abhishek, 2016). For exploring experimental design different independent as well as dependent variables were selected (Table 1). As per the experimental design, a total of 17 formulations were generated and optimized. The selection of independent variables was done based on their ability to affect a formulation. The dependent variables highlighted (Table 1) were chosen as crucial parameters in determining formulation. The above analysis employs 17 runs (Table 2) keeping a center point per

Table 1
List of independent and dependent variables for optimization by BBD.

Independent variables	−1	0	+1
A:Ethyl Cellulose (%w/w)	5	10	15
B:DBS (%w/w)	10	20	30
C:IPM (%w/w)	2.5	5	7.5
Dependent variables	**Goals**		
Y_1:Tensile Strength	Maximize		
Y_2:Water vapor absorption value (WVAV)	Minimize		
Y_3: Drying time	Minimize		

Table 2
Box-Behnken design for the drug-loaded liquid bandage.

Formulation code	SSD (%w/w)	EC concentration (%w/w)	DBS concentration (%w/w)	IPM concentration (%w/w)	Glycerol concentration (%w/w)
LBF1	1	10	10	7.5	1
LBF2	1	10	30	7.5	1
LBF3	1	5	30	5	1
LBF4	1	10	10	2.5	1
LBF5	1	10	20	5	1
LBF6	1	10	20	5	1
LBF7	1	5	20	7.5	1
LBF8	1	5	20	2.5	1
LBF9	1	15	30	5	1
LBF10	1	15	20	2.5	1
LBF11	1	10	30	2.5	1
LBF12	1	10	20	5	1
LBF13	1	15	10	5	1
LBF14	1	10	20	5	1
LBF15	1	5	10	5	1
LBF16	1	10	20	5	1
LBF17	1	15	20	7.5	1

block 1 and the equation created by the software is given as follows:

$$Y = \beta_0 + \beta_1 A + \beta_2 B + \beta_3 C + \beta_{12} AB + \beta_{13} AC + \beta_{23} BC + \beta_{11} A^2 + \beta_{22} B^2 + \beta_{33} C^2$$

In the above equation, the response of the dependent variable is indicated by Y; β_0 is the intercept, and β_1 *to* β_{33}indicates the regression coefficient.

The concentration of EC (A), DBS (B), and IPM (C) were chosen as the independent variables to be involved in the study while the dependent variables were tensile strength (Y_1), water vapor absorption value (Y_2), and drying time (Y_3). Statistical analysis using analysis of variance (ANOVA) was conducted to interpret the outcome of the results.3D response graphs were also generated employing the software design (Sharma, et al., 2022).

2.4. Characterization of film forming system

2.4.1. Physical Appearance, pH, and viscosity

Uniformity, integrity, color, and clarity were determined by visual method. The pH measurements were carried out by using a pre-calibrated digital-type pH meter at room temperature by contacting the surface of the liquid bandage. The brookfield digital viscometer was employed to determine the viscosity of optimized formulation using specific spindle RV-2 (Suresh and Abhishek, 2016).

2.4.2. Tensile strength and drying time

A tensile tester was employed for the evaluation of the mechanical properties of the films following the guidelines of ASTM D882-02. According to these guidelines the tensile strength of the film can be determined with the thickness of less than 1 mm. The constant-rate-of-grip separation test and static weighing test are the techniques which uses constant rate of separation between the grips holding the test specimen's end. Briefly, samples were cut into the rectangle shape and tested with cross head speed of 1 mm/minute. The following formula was employed for the determination of tensile strength:-

$$\text{Tensile Strength } (N/mm^2) = \text{Nbreak}/A \text{ sample}$$

Where N break belongs to the force (Maximum) required for breaking the film and A sample is cross section area of sample (mm^2).

To determine drying time, a glass slide test was followed. The formulated preparation was sprayed on the volunteer's underside of the arm. A glass slide was gently put on film 5 min post spraying. Once removed, if the glass slide had no liquid visible after removal, the film was termed dry. However, if there was some liquid, the process was carried out again with a drying duration of 7 min rather than 5 min (Febriyenti et al., 2010).

2.4.3. Percent moisture uptake

To check the water resistance capacity of a film, an approximately 100 µl sample was evenly sprayed onto the glass plate and was left to dry at a temperature of 25 ± 2 °C. Subsequently, the dried film was weighed and introduced into a water bath (HICON, New Delhi, India) held at a constant temperature of 37 °C.After a period of 24 h, the film was taken out, gently wiped with tissue paper, and reweighed and examined (Aggarwal et al., 2022 & Walendziak et al., 2021) using the formula:

$$\%\ moisturecontent = \frac{\boldsymbol{Ww - Wd}}{\boldsymbol{Ww}} \times\ 100$$

Where Ww = Wet weight.
Wd = Dry weight.

2.4.4. Stickiness of liquid bandage

The assessment of outward stickiness was carried out by applying cotton wool to the dry film under very slight pressure (Süntar et al., 2013). The stickiness was assessed as high (densely accumulated), medium (few fibers), or low (no or occasional fibers) based on the amount of fibers that adhere to the film (Lodhi et al., 2016).

2.4.5. In-vitro release studies

To compare the medication discharge profile from the optimized formulation and marketed formulation (Madecassol), *in-vitro* drug release investigations were carried out utilizing a Franz diffusion cell. The films generated by spraying at a consistent period were sliced into 1 cm^2 and deposited on a pre-treated cellulose acetate membrane to conduct the *in-vitro* drug release investigations. The membrane was fixed to the diffusion cell with the drug-discharging surface of the film facing the receptor compartment (Tas et al., 2003). The receptor compartment was filled with phosphate buffer (PBS) of pH 5.8 at a temperature of 37 ± 0.5 °C and stirred magnetically at a speed of 100 rpm. A sample of the dissolving media (2 ml) was extracted and replaced with a new dissolution medium at each time interval. The percent drug release from the withdrawn samples was determined by Ultra Violet Spectrophotometer (UV). The obtained data was subsequently subjected to fitting against multiple mathematical models, including zero-order, first-order, second-order, Higuchi, and Korsmeyer-Peppas models. Among these models, the formulation exhibiting the highest R^2 value was determined to be the most suitable model for describing drug release behavior.

2.4.6. Excision model for wound healing

For wound healing studies, a total of 18 animals were randomly divided into three groups consisting of 6 animals in each group. Ketamine hydrochloride (40 mg/kg) was given intraperitoneally to

anesthetize the animals and hairs were removed from the dorsal area of the rat by shaving using the electric clippers. A circular wound (8 mm) was induced in each animal using a biopsy punch in the shaved area of rats. Group-I served as the control group (CG) and was allowed to heal naturally without any treatment. Animal group II was treated with the marketed formulation (Madecassol) and the group III was treated with the developed optimized formulation. The marketed formulation contains Centella asiatica, a plant belonging to the Umbelliferae family, is the source of madecassol extract. Asiatic acid, asiaticoside, and madecassic acid are present. It has been applied topically as a wound-healing agent and to stop scarring. The progression in the healing of the wound was photographed on the 0th, 7th, 14th, and 21st day of treatment by the camera and using a caliper. Every morning and evening all test materials were administered (Liu et al., 2010).

2.4.7. Histological study

The animals were anesthetized, following which wound sections were excised for subsequent histological analysis on day 21st of the wound healing study from control group, marketed formulation group and optimized formulation treated group. The extracted tissue samples were subjected to staining using hematoxylin and eosin (H&E) and were examined under a microscope at 40X magnification. Throughout the histology study, factors such as re-epithelialization, the formation of granulation tissue, and the process of angiogenesis were taken into account. These criteria formed the basis for analyzing the microscopic tissue samples and determining the severity of the observed histopathological changes.

2.4.8. Stability studies

As per the guidelines given by the international council of harmonization of technical requirement of pharmaceuticals for human use (ICH), stability studies were performed for liquid bandage optimized formulation. The optimized liquid bandage formulation was filled in the collapsible tube and kept in the different temperature and humidity conditions. To carry out the stability study, the optimized formulation was stored at 25 °C ± 2 °C and 60 ± 5 % relative humidity (RH) and 30 °C ± 2 °C and 65 ± 5 % RH for three months. The formulation was evaluated for physical characteristics, viscosity, drying time, and tensile strength (Gowda et al., 2016).

3. Results and discussion

3.1. Compatibility study by FTIR and DSC

3.1.1. Fourier transform infrared spectroscopy (FTIR)

FTIR spectra of pure drug, drug-polymer physical mixture of bandage formulation is given in Fig. 1.

The FTIR spectrum shows the S═O stretch at 1016.49 cm^{-1}, C—O stretch at 1259.52, C═C stretch at 1661.07 and N—H stretch at 3263.56. The FTIR spectra of both pure drug and drug-polymer physical mixture were preserved, showing that there is no chemical interaction between the drug and the polymers. The results for the FTIR studies were found to match with the reference spectra given by Thampy (2022).

3.1.2. Differential scanning calorimetry

The DSC thermograph of pure drug and physical mixture is shown in Fig. 2. The DSC thermograph of SSD elucidated a pronounced endothermic peak at 300.86 °C. The DSC of the pure drug was found to match with reported results (299.20) by Yassue-Cordeiro et al., 2019. No significant interaction of the drug was observed in the physical mixture and found compatible with other components used in the development of liquid bandage.

3.2. Characterization and fitting of data to the model

The 3-factor 3-level BBD was employed to study the impact of formulation variables on tensile strength (Y_1), water vapour absorption value (Y_2) and drying time (Y_3). A series of experimental runs were generated for the application of Response Surface Methodology (RSM) and the responses thus obtained were enlisted in Table 3.

The models, including first order, second-order, and quadratic models, were fitted to all responses. All three of the observed responses

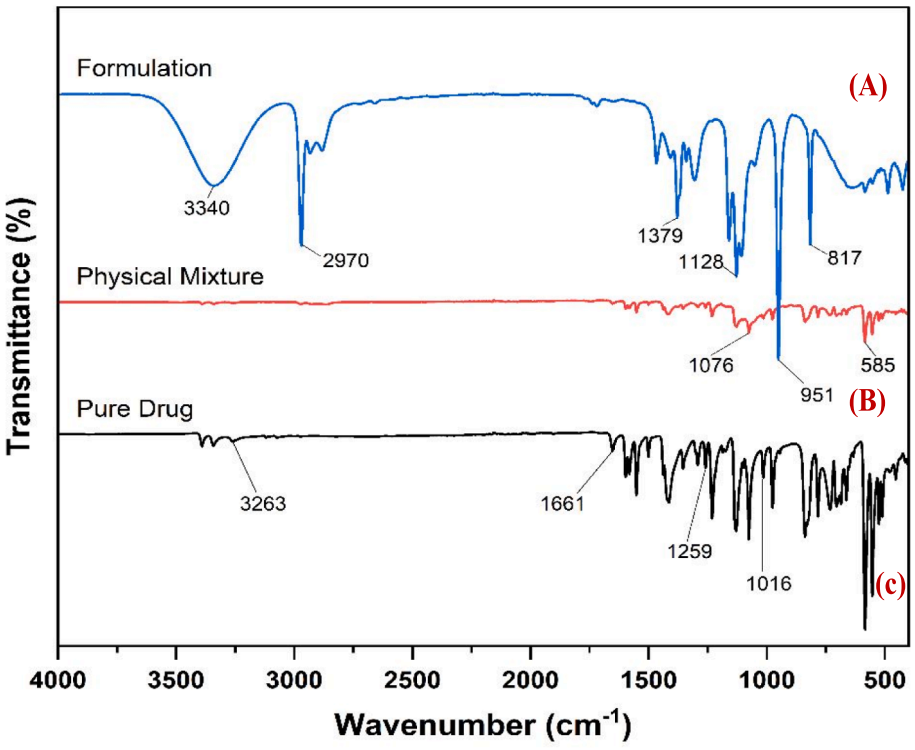

Fig. 1. FTIR spectra of (A) optimized liquid bandage formulation (B) drug-polymer physical mixture (C) Pure drug SSD.

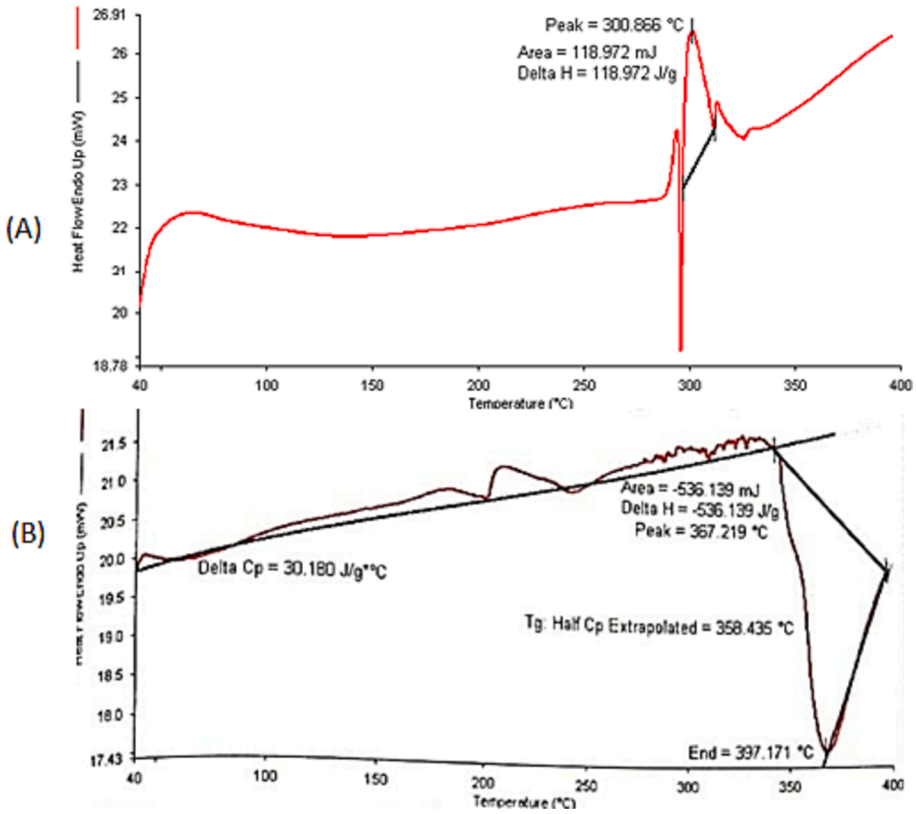

Fig. 2. DSC thermogram of pure drug SSD (A) and physical mixture (B).

Table 3
Drying time, tensile strength, and water vapour absorption value for liquid bandage formulations.

Formulation code	Drying time (min)	Tensile strength (MPa)	Water vapour absorption value (%)
LBF1	2.12 ± 0.5	64.01 ± 1.20	2.10 ± 0.15
LBF2	2.75 ± 0.12	63.05 ± 1.37	2.04 ± 0.05
LBF3	3.00 ± 0.40	63.43 ± 0.55	2.04 ± 0.11
LBF4	2.12 ± 0.11	63.44 ± 0.15	2.03 ± 0.14
LBF5	2.10 ± 0.14	65.21 ± 1.04	2.04 ± 0.45
LBF6	2.50 ± 0.44	67.14 ± 1.40	2.04 ± 0.24
LBF7	2.71 ± 0.17	65.78 ± 0.77	2.09 ± 0.23
LBF8	3.05 ± 0.14	65.78 ± 1.20	2.04 ± 0.22
LBF9	2.37 ± 0.20	67.47 ± 1.00	2.10 ± 0.11
LBF10	2.12 ± 1.25	66.74 ± 0.54	2.04 ± 0.01
LBF11	1.75 ± 0.14	68.24 ± 0.24	2.00 ± 0.25
LBF12	2.56 ± 0.22	66.35 ± 0.45	2.10 ± 0.17
LBF13	1.50 ± 0.35	64.05 ± 1.02	2.04 ± 0.21
LBF14	2.5 ± 0.54	66.35 ± 1.04	2.24 ± 0.05
LBF15	2.09 ± 1.08	63.47 ± 1.36	2.10 ± 0.04
LBF16	2.53 ± 0.24	66.35 ± 1.05	2.04 ± 0.01
LBF17	2.12 ± 0.41	66.74 ± 1.05	2.11 ± 0.14

were found to match most accurately into the quadratic model based on higher R^2 values and minimal expected residual error sum of squares (Prob > F value $p < 0.0001$). The higher standard error values for the coefficients signify that the nature of the relationship is quadratic. ANOVA was performed to investigate the significant differences among the independent variables A, B, and C.

The significance of the model terms was evident from the Prob > F values being lesser than 0.050. The model F-values for variables Y_1, Y_2 and Y_3 were 5.13, 4.79, and 26.71, respectively, indicating that the models were significant. For Y_1, significant model terms included A, B, C, AB, AC, BC, A^2, B^2, and C^2. For Y_2, the significant model terms were A, B, and C, and for Y_3, the significant model terms were A, B, C, AB, AC, BC, A^2, B^2, and C^2. The lack of fit F-values for Y1 was 3.08, for Y_2, 0.59 and 6.24 for Y_3, implying that the lack of fit was not statistically significant in comparison to the level of pure error. The polynomial coefficients demonstrated a good fit to the data, resulting in a predicted R^2 value that closely matched the adjusted R^2 value. The relationship between the independent variables and their responses was established through a polynomial equation, and statistical analysis was conducted using design software (Stat-Ease Inc., Minneapolis, USA). In the equation, positive signs indicated additive effects favoring optimization while responses associated with negative terms indicated detrimental outcomes.3D plots showing the effect of independent variables on dependent variables are given in Fig. 3. Below are given the polynomial Eqs. (1), Eq. (2), and Eq. (3) along with plots depicting the responses Y_1, Y_2, and Y_3 are given below-

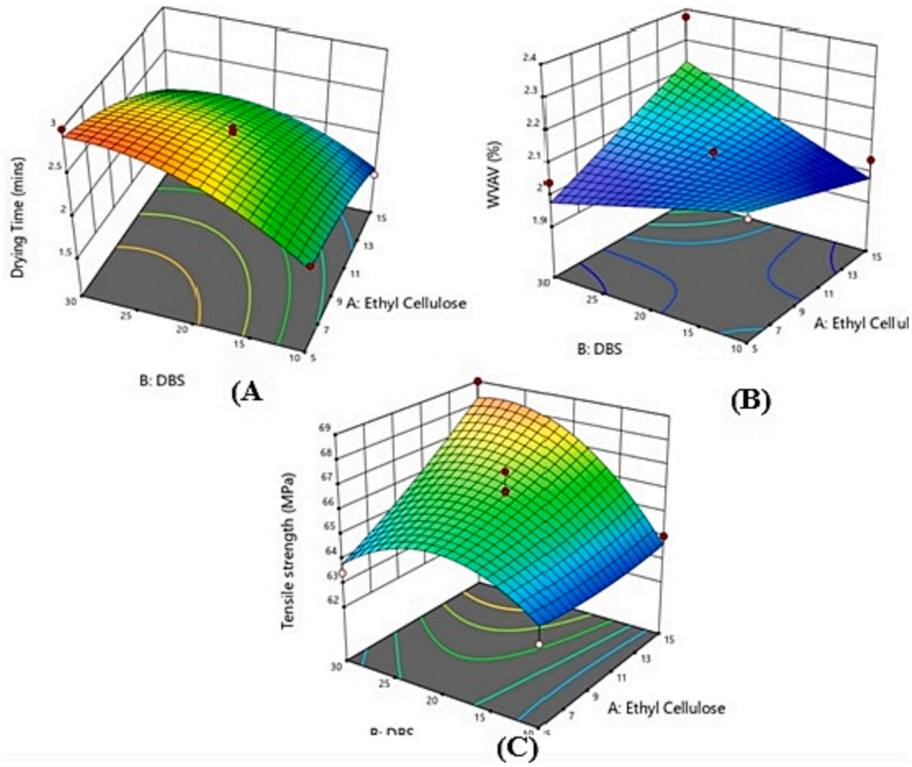

Fig. 3. 3-dimension plots showing impact of independent variables on dependent variables (A) effect of EC and DBS on drying time (B) effect of EC and DBS on water vapour evaporation value (C) effect of EC and DBS on tensile strength.

$$Y_1(\text{tensile strength}) = +66.21 + 1.06A + 1.18B - 0.50C + 1.14AB + 0.00AC - 1.50BC + 0.20A^2 - 1.56B^2 - 0.15C^2 \quad (1)$$

$$Y_2(\text{water vapour absorption value}) = +2.06 - 0.012A - 0.020B + 0.022C \quad (2)$$

$$Y_3(\text{drying time}) = +2.49 - 0.33A + 0.38B - 0.037C - 8.75AB + 0.075AC + 0.00BC - 0.10A^2 - 0.15B^2 + 0.095C^2 \quad (3)$$

For response Y_1, the positive value of A and B in equation (1) indicates that the tensile strength increases as the concentration of ethyl cellulose increases while the negative coefficients of C indicate that tensile strength decreases as the concentration IPM increases. For response Y_2, the water vapor absorption value decreases with an increase in the concentration of factors A and B while positive values were obtained with factor C. For response Y_3, it was found that there was decrease in the drying time with increasing the independent factor A and C while opposite results were obtained with factor C. The formulation code LBF11 was found to be optimized formulation with independent variables concentration of EC, DBS, and IPM as 10, 30, and 2.5 (%w/w) respectively. The tensile strength, water vapor absorption value, and drying time for the optimized liquid bandage formulation were found to be 68.24 ± 0.24, 2.00 ± 0.25 and 1.75 ± 0.14 respectively.

3.2.1. Evaluation of physical characteristics of liquid bandage

The formulation was found to be clear, uniform and transparent without outward stickiness. The viscosity was found to be 60 Cps and with this viscosity, the liquid bandage formulation was suitable to apply as it adheres and spreads well on the skin. The pH observed was 6.0 ± 0.5 which falls within the slightly acidic to neutral range and doesn't cause any skin irritation.

3.2.2. In-vitro release studies

The *in vitro* study shows that the discharge of test formulations was revealed to be higher than the marketed formulation. The results indicated that the drug loaded liquid bandage film initially showed rapid drug release and then throughout the later hours of the study, sustained release was observed Fig. 4.

$$\%\ \text{Cumulative drug release (CDR)} = \frac{\text{Amt of the drug in the sample}}{\text{Amt of the drug in the donor compartment}} \times 100$$

After 6 h of study, the liquid bandage and marketed formulation showed 41.02 % and 29.32 % of drug release respectively. The drug release was found to be significantly higher than the than marketed formulation (White and Turner, 2019).

3.2.3. In vivo wound healing studies

Differentiation of wound area photographed on days 0, 7, 14, and 21^{ist} day for optimized formulation, marketed formulation, and control group were depicted in Fig. 5 and Fig. 6.

Upon comparison with the control group, rats treated with the optimized formulation exhibited a noticeable improvement in wound contraction, showing progressive healing over time. Initially the wound

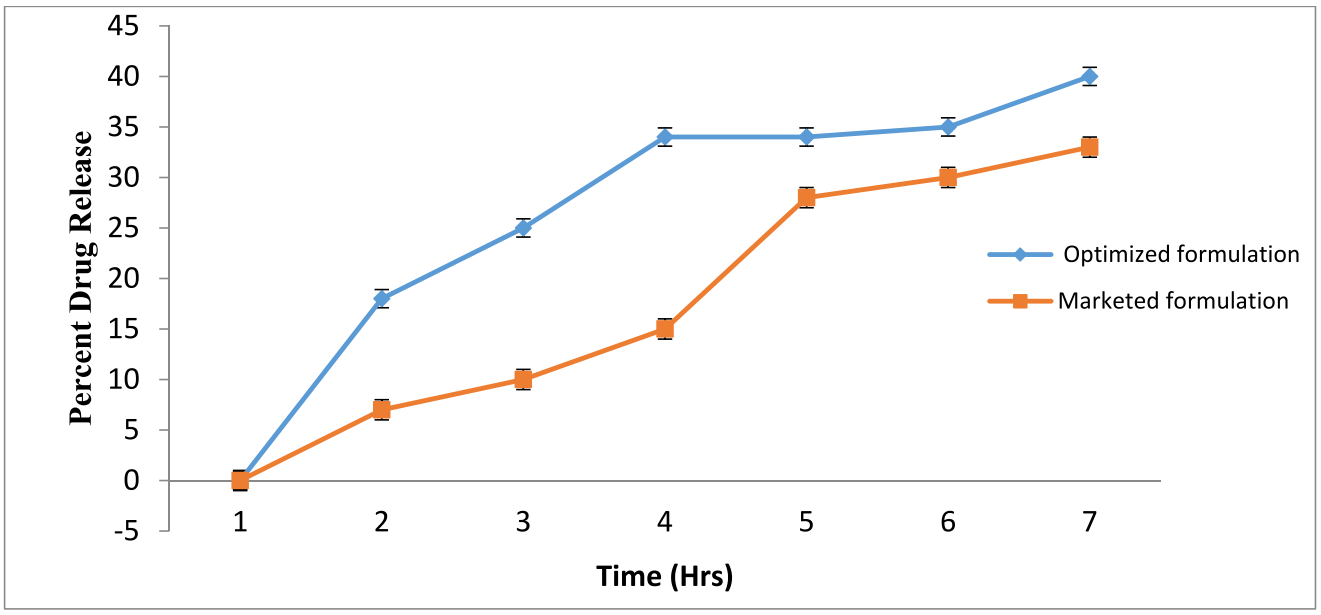

Fig. 4. Cumulative amount of drug release from non pressurized liquid bandage and marketed formulation.

diameter was 8 mm and found to reduce maximum at the day 21st with the optimized formulation (0.8 mm) and followed by marketed formulation (1.44 mm) and normal control group (2.61 mm). In case of the optimized formulation scar left were very light than compared to the marketed formulation and normal control. From the wound healing pattern, it was ascertained that the liquid bandage formulation was more effective than the marketed formulation and there is noticeably greater healing compared to the normal control and marketed formulation (Bekta et al., 2020).

3.2.4. *Histological results*

The histological examinations revealed that the optimized liquid bandage formulation played a role in promoting the regeneration of both the epidermal and dermal layers. In the context of the 21st day observation period, rats treated with the formulation displayed a noticeable improvement in re-epithelialization. Upon analysis, it was evident that the formulation-treated groups exhibited significantly superior outcomes when compared to both the control and marketed groups (Fig. 7C). H&E stained sections of the control group (Fig. 7A) showed tissue lined by stratified squamous epithelium, only 2–3 layers thick. Sub-epithelial tissue showed collagenised stroma with skin appendages while only mild fibrosis was found in the subcutaneous tissue. In the marketed group (Fig. 7B), besides stratified squamous epithelium mildpapillomatosis and mild hyperkeratosis were found. Sub-epithelial

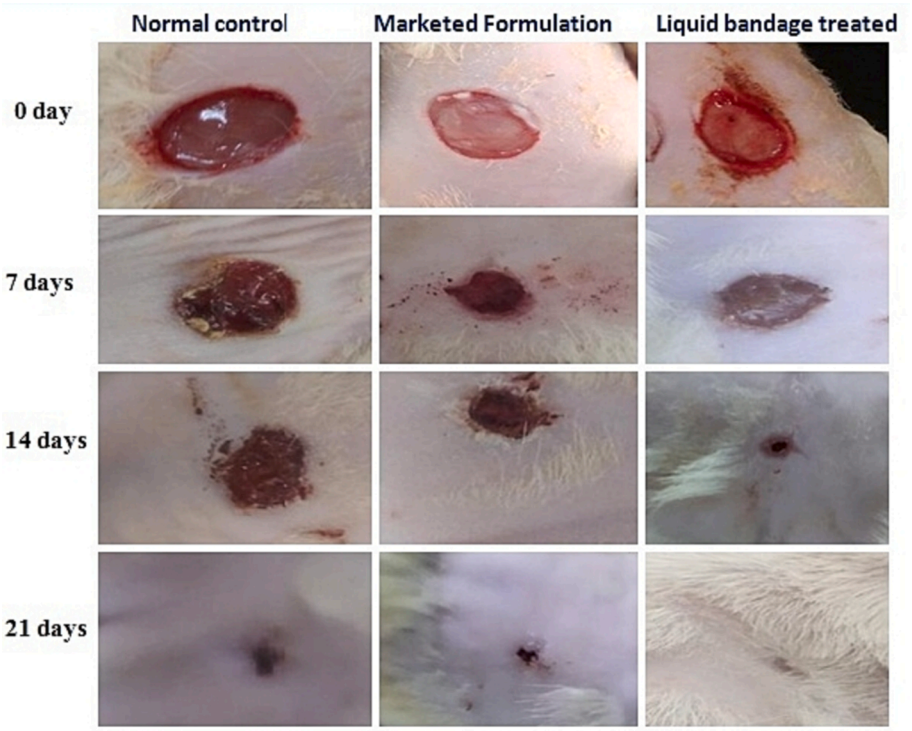

Fig. 5. Photographic representation of experimental wound healing during 0, 7, 14, and 21 days post-surgery.

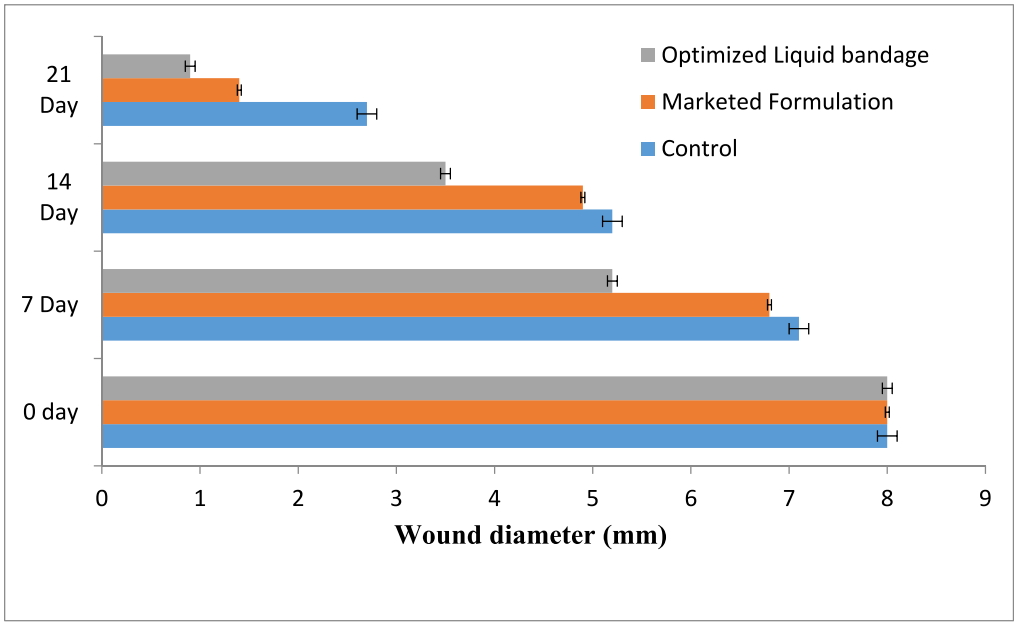

Fig. 6. Wound construction of optimized liquid bandage, marketed formulation, and normal control on day 0 day 1, day 7, day 14, and day 21.

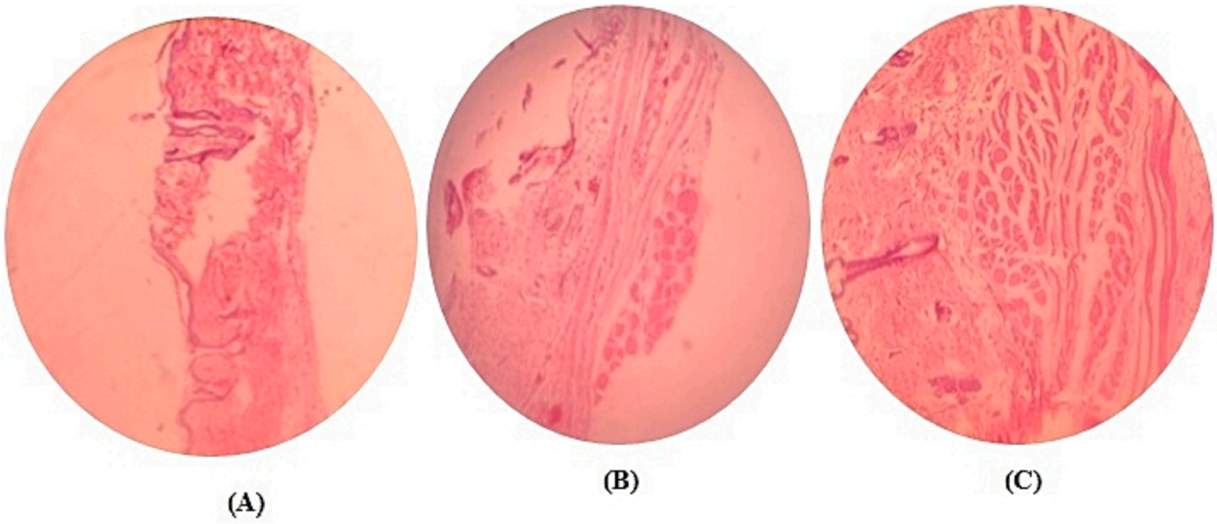

Fig. 7. Histological analyses of healed skin tissues from wound area (A) Normal control (B) Marketed formulation treated (C) Optimized formulation treated.

tissue is thicker, and showed more collagenised stroma with many skin appendages while the subcutaneous tissue showed more fibrosis compared to control. The H&E stained sections of the formulation group showed more papillomatosis and mild hyperkeratosis as compared to control and marketed group. Sub-epithelial tissue is thicker, and shows more collagenised stroma with many skin appendages. There is higher vascular proliferation and shows *peri*-appendageal lymphoplasmacytic infiltrate. Subcutaneous tissue showed more fibrosis compared to the control and marketed group. Overall, the optimized formulation showcased its ability to expedite re-epithelialization and wound healing. This finding indicates its potential in enhancing the regenerative processes of the skin's epidermal and dermal layers.

3.2.5. *Stability studies*

After the three month of stability study, the film was clear and transparent in appearance with high water capacity and no changes in observed drying time.

3.3. *Discussion*

Wound healing is an impulsive and intricate physiological process (Cañedo-Dorantes and Cañedo-Ayala, 2019) that coordinates with the advancement of healing through the several discrete wound healing phases (Desmet,et al., 2018). These phases of wound healing [Fig. 1] include the release of different growth factors (GF), cytokines, phagocytosis, chemotaxis, remodeling of collagen, synthesis of neo-collagen, and breakdown of collagen (Eming,et al., 2014). The four separate but linked phases of wound healing are hemostasis, inflammation, proliferation, and tissue remodeling. Initially, during hemostasis platelets assemble together to stop the bleeding which causes the vessels to constrict and results in scab formation (Wallace,et al., 2017). The platelets travel to the wound location and aid in blood clotting without obstructing the regular flow of blood. This procedure also regulates microbial dissemination following an injury (El Ashram,et al., 2021). The phase of inflammation that follows hemostasis witnesses immune cells (monocytes, lymphocytes, neutrophils, and macrophages)

migration towards the site of the injury as a result of damage indication signals to ward off microbial infection. This phase is characterized by the release of a number of growth factors like platelet-derived (PDGF), fibroblast (FGF), epidermal (EGF), and transforming growth factor and cytokines, together with tumor necrosis factor (TNF), interleukin (IL)-1,6, and 17 (Kanji and Das, 2017). Neutrophils first reach the wound area and stay there for 24 h after starting the healing process. Interleukin-17, a neutrophils cytokine, and vascular endothelial growth factor, a secreted growth factor, mediate the migration of other immune cells in order to maintain the ongoing digestion of leftover debris and bacteria for skin regeneration (Wu et al., 2015). After an injury, the inflammatory phase lasts for one to four days and cleans out the wound's material through phagocytosis (Zhao et al., 2016). The growth factors and cytokines attract several additional cells, inclusive of fibroblasts, keratinocytes, stem/progenitor, and endothelial cells (Barchitta et al., 2019). The *in vitro* and *in vivo* studies conducted in this research provide valuable insights into the effectiveness of the developed liquid bandage formulation for wound-healing. The *in vitro* drug release study indicated that the test formulations exhibited a higher cumulative drug release compared to the marketed formulation. This suggests that the drug-loaded liquid bandage film initially releases the drug rapidly, which is followed by a sustained release over an extended period. This controlled drug release profile can be advantageous in maintaining a therapeutic drug concentration at the wound site, potentially promoting efficient wound healing. For the *in vivo* wound healing studies, the differentiation of wound areas over the course of 21 days was monitored. The photographic representation of wound healing patterns demonstrated that rats treated with the optimized formulation showed significant improvement in wound healing compared to both the control group and the group treated with the marketed formulation. The observation of progressive healing over time in the optimized formulation group suggests its ability to accelerate the wound healing process. This outcome aligns with the desired attributes of a wound healing agent, emphasizing the potential superiority of the liquid bandage formulation over conventional approaches. The histological examination provided deeper insights into the regenerative effects of the liquid bandage. The optimized formulation was found to play a substantial role in promoting the regeneration of both the epidermal and dermal layers of the skin. The histological sections displayed enhanced re-epithelialization in the formulation-treated groups compared to the control and marketed groups. This further underscores the formulation's capability to facilitate tissue repair and regeneration, indicating its potential to foster a favorable wound healing environment. The histological sections also revealed certain distinctive characteristics within each group. In the control group, tissue lining exhibited stratified squamous epithelium with limited thickness. The marketed group displayed mild papillomatosis and hyperkeratosis, along with increased collagenized stroma and skin appendages. However, the formulation group showed higher vascular proliferation and a *peri*-appendageal lymphoplasmacytic infiltrate, suggesting a more active regenerative response. The application of non-pressurized liquid bandage formulations containing SSD, according to the authors, may open up new avenues for the treatment of wounds and benefit contemporary medicine because topical medications for wound healing are currently limited in supply and may result in unfavorable allergic skin reactions.

4. Conclusion

In the current study, the liquid bandage was successfully developed, optimized, and evaluated. Among the innovative formulations for applying to injured skin, film-based liquid bandages have demonstrated advantages because they can create a damp environment for wounds while also delivering integrated medicine to the wound site. Owing to its broad spectrum of action against germs, SSD is the medication of choice for wound therapy. Overall, the results suggest that the developed film-forming liquid bandage with SSD has great potential as a wound-healing medicament and can be a promising alternative to conventional wound dressings.

Declaration of competing interest

The authors declare that they have no known competing financial interests or personal relationships that could have appeared to influence the work reported in this paper.

Acknowledgment

The authors are thankful to the Researchers Supporting Project number (RSPD2023R568), King Saud University, Riyadh, Saudi Arabia.

References

Abd El-Kader, M.F.H., Elabbasy, M.T., Ahmed, M.K., Menazea, A.A., 2021. Structural, morphological features, and antibacterial behavior of PVA/PVP polymeric blends doped with silver nanoparticles via pulsed laser ablation. J. Mater. Res. Technol. 13 https://doi.org/10.1016/j.jmrt.2021.04.055.

Abd El-Kader, M.F.H., Ahmed, M.K., Elabbasy, M.T., Afifi, M., Menazea, A.A., 2021. Morphological, mechanical and biological properties of hydroxyapatite layers deposited by pulsed laser deposition on alumina substrates. Surf. Coat. Technol. 409, 126861 https://doi.org/10.1016/j.surfcoat.2021.126861.

Aggarwal, S., Thakur, A., Sharm, A., 2022. Development and evaluation of ketoprofen loaded floating microspheres for sustained delivery. Mater. Today:. Proc. 68, 647–652.

Aldalbahi, A., Ahmed, M.K., Govindasami, P., Rahaman, M., Anter, A., 2020. Core–shell Au@Se nanoparticles embedded in cellulose acetate/polyvinylidene fluoride scaffold for wound healing. J. Mater. Res. Technol. 9, 15045–15056. https://doi.org/10.1016/j.jmrt.2020.10.079.

Anter, A., Ismail, A.M., Samy, A., 2021. Novel green synthesis of zinc oxide nanoparticles using orange waste and its thermal and antibacterial activity. J. Inorg. Organomet. Polym Mater. 31, 1–10. https://doi.org/10.1007/s10904-021-02074-2.

Atiyeh, B.S., Costagliola, M., Hayek, S.H., Dibo, S.A., 2007. Effect of silver on burn wound infection control and healing: a review of the literature. Burns 33, 139–148.

Aziz, Z., Abu, S.F., Chong, N.J., 2012. A systematic review of silver-containing dressings and topical silver agents (used with dressings) for burn wounds. Burns 38 (3), 307–318. https://doi.org/10.1016/j.burns.2011.09.020.

Barchitta, M., Maugeri, A., Favara, G., Lio, R.M.S., Evola, G., Agodi, A., Basile, G., 2019. Nutrition and wound healing: an overview focusing on the beneficial effects of curcumin. Int. J. Mol. Sci. 20, 1119.

Brown, S.M., Davis, E.R., 2019. Statistical optimization of liquid bandage formulation for wound care. Pharm. Formulation Sci. 8 (2), 56–71.

Cañedo-Dorantes, L., Cañedo-Ayala, M., 2019. Skin acute wound healing: a comprehensive review. Int. J. Inflflam. 2019, 3706315.

Desmet, C.M., Préat, V., Gallez, B., 2018. Nanomedicines and gene therapy for the delivery of growth factors to improve perfusion and oxygenation in wound healing. Adv. Drug Deliv. Rev. 129, 262–284.

Dhivya, S., Padma, V.V., Santhini, E., 2015. Wound dressings—a review. Biomedicine 5, 22.

Edlich, R.F., Rodeheaver, G.T., Thacker, J.G., Lin, K.Y., Drake, D.B., Mason, S.S., 1978. Silver sulfadiazine: therapy for burn wound infections. Ann. Surg. 188 (2), 228–239. https://doi.org/10.1097/00000658-197808000-00016.

El Ashram, S., El-Samad, L.M., Basha, A.A., El Wakil, A., 2021. Naturally-derived targeted therapy for wound healing: beyond classical strategies. Pharmacol. Res. 170, 105749.

El-Newehy, M., Anter, A., Thamer, B., Elnaggar, M., 2021. Preparation of antibacterial film-based biopolymer embedded with vanadium oxide nanoparticles using one-pot laser ablation. J. Mol. Struct. 1225, 129163.

Eming, S.A., Martin, P., Tomic-Canic, M., 2014. Wound repair and regeneration: mechanisms, signaling, and translation. Sci. Transl. Med. 6, 265.

Fathi, A., Ahmed, M., Afifi, M., Anter, A., Uskokovic, V., 2020. Taking hydroxyapatite-coated titanium implants two steps forward: surface modification using graphene mesolayers and a hydroxyapatite-reinforced polymeric Scaffold. ACS Biomater Sci. Eng. 7 https://doi.org/10.1021/acsbiomaterials.0c01105.

Gowda, D.V., Suresh, J., Ram, A., Srivastava, A., 2016. Formulation and evaluation of topical gel using Eupatorium glandulosum michx for wound healing activity. Der Pharmacia Letter. 8 (8), 255–266.

Jodar, K.P.S., Balc, V.M., Chaud, V.M., Tubino, M., Yoshida, V.M.H., Oliveira, M.J., et al., 2015. Development and characterization of a hydrogel containing silver sulfadiazine for antimicrobial topical applications. J. Pharm. Sci. 104, 2241–2251.

Kanji, S., Das, H., 2017. Advances of stem cell therapeutics in cutaneous wound healing and regeneration. Mediat. Inflamm. 2017, 5217967.

Kim, D.W., Kim, K.S., Seo, Y.G., Lee, B.J., Park, Y.J., Youn, Y.S., et al., 2015. Novel sodium fusidate-loaded film-forming hydrogel with easy application and excellent wound healing. Int. J. Pharm. 495, 67–74.

Liu, X., Lee, P.Y., Ho, C.M., Lui, V.C., Chen, Y., Che, C.M., et al., 2010. Silver nanoparticles mediate differential responses in keratinocytes and fibroblasts during skin wound healing. Chem. Med. Chem. 5, 468–475. https://doi.org/10.1002/cmdc.200900502.

Lodhi, S., Jain, A.P., Rai, G., Yadav, A.K., 2016. Preliminary investigation for wound healing and anti-inflammatory effects of Bambusa vulgaris leaves in rats. J. Ayurveda Integr. Med. 7 (1), 14–22. https://doi.org/10.1016/j.jaim.2015.07.001.
Monavarian, M., Kader, S., Moeinzadeh, S., Jabbari, E., 2019. Regenerative scar-free skin wound healing. Tissue Eng. Part B Rev. 25, 294–311.
Morsi, N.M., Abdelbary, G.A., Ahmed, M.A., 2014. Silver sulfadiazine based cubosome hydrogels for topical treatment of burns: development and in vitro/in vivo characterization. Eur. J. Pharm. Sci. 86, 178–189.
Pereira, G.G., Guterres, S.S., Balducci, A.G., Colombo, P., Sonvico, F., 2014. Polymeric films loaded with vitamin E and Aloe vera for topical application in the treatment of burn wounds. Biomed. Res. Int. 2014, 1–9.
Raja, S.K., Garcia, M.S., Isseroff, R.R., 2007. Wound re-epithelialization: modulating keratinocyte migration in wound healing. Front. Biosci. (landmark Ed) 12, 2849–2868.
Ranade, S., Bajaj, A., Londhe, V., Kao, D., Babul, N., 2014. Fabrication of polymeric film forming topical gels. Int. J. Pharm. Sci. Rev. Res. 26 (2), 306–313.
Robson, M.C., 1997. Wound infection: a failure of wound healing caused by an imbalance of bacteria. Surg. Clin. North. Am. 77, 637–650.
Robson, M.C., Steed, D.L., Franz, M.G., 2001. Wound healing: biologic features and approaches to maximize healing trajectories. Curr. Probl. Surg. 38, 72–140.
Rodeheaver, G.T., Pettry, D., 1976. Silver sulfadiazine: in vitro antibacterial activity. Antimicrob Agents Chemother. 10 (5), 768–772. https://doi.org/10.1128/aac.10.5.768.
Sharma, A., Harikumar, S.L., 2020. Quality by design approach for development and optimization of nitrendipine-loaded niosomal gel for accentuated transdermal delivery. Int. J. Appl. Pharm. 12 (5), 181–189. https://doi.org/10.22159/ijap.2020v12i5.38639.
Sharma, A., Singh, A.P., Harikumar, S.L., 2020. Development and optimization of nanoemulsion based gel for enhanced transdermal delivery of nitrendipine using box- behnken statistical design. Drug Dev. Ind. Pharm. 46 (2), 329–342. https://doi.org/10.1080/03639045.2020.1721527.
Sharma, A., Thakur, R., Sharma, R., 2022. Development and optimization of candesartan cilexitil nasal gel for accentuated intranasal delivery using central composite design. Mater. Today: Proc. https://doi.org/10.1016/j.matpr.2022.11.221.
Singh, B., Sharma, S., Dhiman, A., 2013. Design of antibiotic-containing hydrogel wound dressings: biomedical properties and histological study of wound healing. Int. J. Pharm. 457, 82–91.
Smith, J.D., Johnson, A.R., 2020. Advanced wound care using silver sulfadiazine-loaded liquid bandages. J. Wound Healing Res. 10 (3), 123–137.
Süntar, I., Küpeli Akkol, E., Keles, H., Yesilada, E., Sarker, S.D., 2013. Exploration of the wound healing potential of Helichrysum graveolens (Bieb.) Sweet: isolation of apigenin as an active component. J. Ethnopharmacol. 149 (1), 103–110. https://doi.org/10.1016/j.jep.2013.06.006.
Suresh, C., Abhishek, S., 2016. pH sensitive in situ ocular gel: a review. J. Pharma Sci. Bioscienti Res. 6 (5), 684–694.
Tas, C., Ozkan, Y., Savaser, A., Baykara, T., 2003. In vitro release studies of chlorpheniramine maleate from gels prepared by different cellulose derivatives. II Farmaco. 58, 605–611.
Thakur, R., Sharma, A., 2019. An overview of mucoadhesive thermoreversible nasal gel. Asian J. Pharm. Res. Dev. 9 (4), 158–168. https://doi.org/10.22270/ajprd.v9i4.994.
Thampy, R., 2022. Development, optimization and evaluation of silver sulphadiazine loaded nano fibrous scafold as wound healing. Int. J. Drug Develop. Res. 14 (10), 978.
Tort, S., Demiröz, F.T., Cevher, S.C., Sarıbaş, S., Özoğul, C., Acartürk, F., 2020. The effect of a new wound dressing on wound healing: biochemical and histopathological evaluation. Burns 46, 143–155.
Tottoli, E.M., Dorati, R., Genta, I., Chiesa, E., Pisani, S., Conti, B., 2020. Skin wound healing process and new emerging technologies for skin wound care and regeneration. Pharmaceutics. 12, 735.
Venkataraman, M., Nagarsenker, M., 2013. Silver sulfadiazine nanosystems for burn therapy. AAPS Pharm. Sci. Tech. 14 (1), 215–223.
Vij, N.N., Saudagar, R.B., 2014. Formulation, development, and evaluation of film-forming gel for prolonged dermal delivery of terbinafine hydrochloride. Indian J. Pharm. Sci. Res. 5 (9), 537–554.
Walendziak, W.P., Kozlowska, J., 2021. Design of sodium alginate/gelatin-based emulsion film fused with polylactide microparticles charged with plant extract. Materials 14, 745. https://doi.org/10.3390/ma14040745.
Wallace, H.A., Basehore, B.M., Zito, P.M., 2017. Wound Healing Phases; StatPearls Publishing: Treasure Island, FL, USA.
White, A.L., Turner, B.S., 2019. Enhanced drug release in liquid bandages for efficient wound healing. Int. J. Pharm. Sci. 11 (2), 87–101.
Wu, L., Chen, X., Zhao, J., Martin, B., Zepp, J.A., Ko, J.S., Gu, C., Cai, G., Ouyang, W., Sen, G., et al., 2015. A novel IL-17 signaling pathway controlling keratinocyte proliferation and tumorigenesis via the TRAF4–ERK5 axis. J. Exp. Med. 212, 1571–1587.
Zhao, R., Liang, H., Clarke, E., Jackson, C., Xue, M., 2016. Inflammation in chronic wounds. Int. J. Mol. Sci. 17, 2085.